Available online at www.sciencedirect.com
SCIENCE DIRECT®
C. R. Acad. Sci. Paris, Ser. I 342 (2006) 279–284
COMPTES RENDUS MATHEMATIQUE
http://france.elsevier.com/direct/CRASS1/

Numerical Analysis

A projection algorithm for fluid–structure interaction problems with strong added-mass effect ☆

Miguel A. Fernández, Jean-Frédéric Gerbeau, Céline Grandmont

INRIA, REO team, Rocquencourt, B.P. 105, 78153 Le Chesnay cedex, France

Received 29 March 2005; accepted after revision 7 December 2005

Presented by Olivier Pironneau

Abstract

This Note aims at introducing a semi-implicit coupling scheme for fluid–structure interaction problems with a strong added-mass effect. Our main idea relies on the splitting of added-mass, viscous effects and geometrical/convective non-linearities, through a Chorin–Temam projection scheme within the fluid. We state some theoretical stability results, in the linear case, and provide some numerical experiments. The main interest of the proposed scheme is its efficiency compared to the implicit approach. ***To cite this article: M.A. Fernández et al., C. R. Acad. Sci. Paris, Ser. I 342 (2006).***

Résumé

Un algorithme de projection pour des problèmes d'interaction fluide–structure avec fort effet de masse ajoutée. Dans cette Note nous introduisons un schéma semi-implicite pour des problèmes d'interaction fluide–structure avec un fort effet de masse-ajoutée. La méthode est basée sur un certain découplage de la masse ajoutée, des effets visqueux et des non linéarités géometriques et convectives. Ce découplage peut être obtenu par une méthode de projection type Chorin–Temam. Nous énonçons un résultat de stabilité dans un cadre linéaire, et nous présentons quelques simulations numériques. Le principal intérêt de l'algorithme proposé est son efficacité par rapport aux approches implicites. ***Pour citer cet article : M.A. Fernández et al., C. R. Acad. Sci. Paris, Ser. I 342 (2006).***

Version française abrégée

Le but de cette Note est de présenter un schéma semi-implicite stable pour simuler des problèmes d'interaction fluide–structure dans le cas où le fluide est visqueux incompressible et la densité de la structure est proche de celle du fluide (c'est-à-dire, lorsque les effets de masse ajoutée sont importants). C'est le cas par exemple dans les écoulements sanguins. Dans de telles situations, des instabilités numériques ont été observées [6,11,12] lorsque (1) n'est pas vérifiée

☆ This work has been carried out during a one-year *délégation* of C. Grandmont at INRIA, and partially supported by the European Community through the Research Training Network "Mathematical Modelling of the Cardiovascular System (HaeMOdel)", contract HPRN-CT-2002-00270.
E-mail addresses: miguel.fernandez@inria.fr (M.A. Fernández), jean-frederic.gerbeau@inria.fr (J.-F. Gerbeau), grandmont@ceremade.dauphine.fr (C. Grandmont).

1631-073X/$ – see front matter
doi:10.1016/j.crma.2005.12.017

assez précisément, par exemple pour des schémas explicites. On trouvera dans [1,9] des explications théoriques de l'apparition de ces instabilités numériques. Un moyen de palier ces instabilités est de mettre en œuvre des schémas implicites, souvent très coûteux. Ces dernières années de nombreux travaux se sont donc attachés à développer des stratégies efficaces pour réaliser ce couplage « fort » (voir [2,5,6,10]). Ici, nous souhaitons lever la nécessité de ce couplage implicite. L'idée principale est de traiter séparément les efforts de pression et les efforts visqueux appliqués par le fluide sur la structure, les premiers étant traités implicitement comme le suggère [1], les seconds étant traités explicitement ce qui, comme le suggère [7] conduit à des schémas conditionnellement stables. Un des moyens de parvenir à ce traitement implicite-explicite des efforts est d'utiliser un schéma de projection type Chorin–Temam pour résoudre la partie fluide. Ce qui conduit pour le problème couplé (2)–(3) au schéma semi discrétisé en temps (4)–(7). Il est à noter que la convection et les non-linéarités géométriques sont prises en compte à l'étape de diffusion. Pour un tel schéma nous énonçons une propriété de stabilité (Théorème 2.1) et illustrons les capacités de l'algorithme à traiter un cas avec fort effet de masse ajoutée, en l'appliquant au problème de l'écoulement sur une marche avec un fond élastique (Fig. 1).

1. Introduction and motivation

In this Note we are interested in the numerical simulation of fluid–structure interaction problems involving an incompressible fluid in presence of a strong added-mass effect. This issue is particularly difficult to face when the fluid added-mass acting on the structure is strong, in other words, when the fluid and solid densities are of the same order, as it happens in hemodynamics for example. Indeed, as it has been reported in many works, in such situations, *strong* (or implicit) coupling schemes, i.e. preserving energy balance, appeared to be mandatory in order to avoid numerical instabilities. We introduce in this Note a scheme which is not implicit but which is stable for a reasonable range of discretization parameters in standard test cases.

Let $\Omega(t)$ be a time-dependent domain in $\mathbb{R}^d$ ($d = 2$ or 3). We assume, for all time t, that $\overline{\Omega(t)} = \overline{\Omega_{\mathrm{f}}(t)} \cup \overline{\Omega_{\mathrm{s}}(t)}$ and $\Omega_{\mathrm{f}}(t) \cap \Omega_{\mathrm{s}}(t) = \emptyset$, where $\Omega_{\mathrm{f}}(t)$ is occupied by an incompressible viscous fluid and $\Omega_{\mathrm{s}}(t)$ by an elastic solid. The fluid–structure interface is denoted by $\Sigma(t) = \overline{\Omega_{\mathrm{f}}(t)} \cap \overline{\Omega_{\mathrm{s}}(t)}$. Denoting, respectively, the velocity and the Cauchy stress tensor by $\boldsymbol{u}$ and $\boldsymbol{\sigma}_{\mathrm{f}}$ within the fluid and by $\boldsymbol{v}_{\mathrm{s}}$ and $\boldsymbol{\sigma}_{\mathrm{s}}$ in the structure, the fluid–structure coupling is performed by imposing the transmission conditions

$$\boldsymbol{u} = \boldsymbol{v}_{\mathrm{s}}, \quad \boldsymbol{\sigma}_{\mathrm{f}} \cdot \boldsymbol{n}_{\mathrm{f}} + \boldsymbol{\sigma}_{\mathrm{s}} \cdot \boldsymbol{n}_{\mathrm{s}} = 0, \quad \text{on } \Sigma, \tag{1}$$

where $\boldsymbol{n}_{\mathrm{f}}$ (resp. $\boldsymbol{n}_{\mathrm{s}}$) stands for the outward normal on $\partial\Omega_{\mathrm{f}}$ (resp. $\partial\Omega_{\mathrm{s}}$).

Many fluid–structure interaction problems can be discretized through a 'weak' coupling of the fluid and structure sub-problems. Indeed, stable schemes can be obtained without the need of enforcing (1) accurately at each time step. A state-of-the-art presentation of such algorithms can be found in [3]. However, in some situations, numerical instabilities, irrespective of the time step, may occur. This fact has been observed in many numerical studies (for instance [6,11,12]), and some theoretical explanations have been proposed in [1,9]. In particular, in [1], it has been shown that, for incompressible fluids, instabilities are closely related to similarities between the fluid and solid densities. Up to now, instabilities have been overcome through *strong* coupling. Therefore, at each time step, many 'sub-iterations' have to be performed in order to enforce (1), which often leads to prohibitive computational costs. Thus, most of the recent works have been devoted to the development of efficient methods for the solution of the non-linear problems arising in this implicit coupling (see [2,5,6,10]). Although significant improvements have been achieved, none of the existing strategies are able to circumvent strong coupling without compromising stability, to the authors knowledge.

2. A projection scheme

Our scheme is based on the following two ideas. First, in order to avoid numerical instabilities, the main part of the added-mass effect is implicitly treated, as suggested in [1], whereas the other contributions (dissipation, convection and geometrical non-linearities) are treated explicitly. The second idea, relies on the fact that this kind of implicit-explicit splitting can be optimally performed using a Chorin–Temam projection scheme (see for instance [8]) in the fluid. Indeed, at each time step, the projection sub-step (carried out in a known fluid domain) is implicitly coupled with the structure, so accounting for the added-mass effect, the viscous sub-step, which is explicit (so weakly coupled), takes into account the viscous effects and the convective and geometrical non-linearities. The main advantages of the

resulting algorithm are: its simplicity of implementation (specially compared to sophisticated Newton-like methods [5,6]) and its outstanding efficiency compared to any strong coupling methods we are aware of. Obviously, the main inconvenience is that energy is not perfectly balanced at each time step, at least from a theoretical viewpoint. In despite of that, theoretical and numerical evidences show that, for a reasonable range of physical and discrete parameters, the scheme is numerically stable.

Let $\widehat{\Omega} = \widehat{\Omega}_{\rm f} \cup \widehat{\Omega}_{\rm s}$ be a reference configuration of the system. We define the deformation of the continuum medium by $\boldsymbol{\varphi}: \widehat{\Omega} \times [0,T] \to \Omega(t)$, the deformation gradient by $\boldsymbol{F}(\hat{x},t) = \nabla_{\hat{x}} \boldsymbol{\varphi}(\hat{x},t)$, and its determinant by $J(\hat{x},t) = \det \boldsymbol{F}(\hat{x},t)$. The displacement of the domain is given by $\boldsymbol{\eta}(\hat{x},t) = \boldsymbol{\varphi}(\hat{x},t) - \hat{x}$. Within the structure, the velocity of a material point $\hat{x}$, $\partial_t \boldsymbol{\varphi}(\hat{x},t) = \partial_t \boldsymbol{\eta}(\hat{x},t)$, is denoted by $\boldsymbol{v}_{\rm s}$. Within the fluid, $\boldsymbol{u}(x,t)$ stands for the fluid velocity at a point x of the fluid domain. In addition, we adopt a fluid Arbitrary Lagrangian Eulerian (ALE) formulation by introducing another mapping, $A: \widehat{\Omega}_{\rm f} \times [0,T] \to \Omega_{\rm f}(t)$ such that $A(\cdot,0)_{|\widehat{\Sigma}} = \boldsymbol{\varphi}(\cdot,0)_{|\widehat{\Sigma}}$, which in general does not follows the material trajectories. The fluid domain velocity is defined by $\boldsymbol{w}(\hat{x},t) = \partial_t A(\hat{x},t)$. We introduce the first Piola–Kirchhoff tensor in the structure $\boldsymbol{\Pi} = J(\boldsymbol{\sigma}_{\rm s} \circ \boldsymbol{\varphi}) \boldsymbol{F}^{-\rm T}$. The field $\boldsymbol{\Pi}$ is related to $\boldsymbol{\eta}$ through an appropriate constitutive law. We assume the fluid to be incompressible and Newtonian, thus $\boldsymbol{\sigma}_{\rm f}(p,\boldsymbol{u}) = -p\mathbf{I} + \mu(\nabla \boldsymbol{u} + \nabla \boldsymbol{u}^{\rm T})$ where p denotes the pressure. The fluid–structure problem then reads:

$$\begin{cases} \rho_{\rm f} \dfrac{\partial \boldsymbol{u}}{\partial t}\bigg|_{\hat{x}} + \rho_{\rm f}(\boldsymbol{u} - \boldsymbol{w}) \cdot \nabla \boldsymbol{u} - \mu \Delta \boldsymbol{u} + \nabla p = 0 \quad \text{in } \Omega_{\rm f}(t), \quad \operatorname{div} \boldsymbol{u} = 0 \quad \text{in } \Omega_{\rm f}(t), \\ \boldsymbol{w} = \operatorname{Tr}^{-1}(\boldsymbol{v}_{\rm s}|_{\widehat{\Sigma}}) \quad \text{in } \widehat{\Omega}_{\rm f}, \quad \boldsymbol{u} = \boldsymbol{v}_{\rm s} \circ \boldsymbol{\varphi}^{-1} \quad \text{on } \Sigma(t), \end{cases} \tag{2}$$

$$\begin{cases} \rho_{\rm s} \dfrac{\partial^2 \boldsymbol{\eta}}{\partial t^2} - \operatorname{div}_{\hat{x}}(\boldsymbol{\Pi}) = 0, & \text{in } \widehat{\Omega}_{\rm s}, \\ \boldsymbol{\Pi} \cdot \boldsymbol{n}_{\rm s} = J \boldsymbol{\sigma}_{\rm f}(p,\boldsymbol{u}) \cdot \boldsymbol{F}^{-\rm T} \cdot \boldsymbol{n}_{\rm s}, & \text{on } \widehat{\Sigma}, \end{cases} \tag{3}$$

where $\frac{\partial}{\partial t}|_{\hat{x}}$ represents the ALE time derivative and Tr^{-1} denotes any reasonable extension operator in the fluid domain (see, e.g., [9]).

Assuming Ω^n, $\boldsymbol{u}^n$, p^n, $\boldsymbol{\eta}^n$ to be known, our scheme reads as follows:

– **Step 1:** Extrapolation of the domain: $\Omega_{\rm f}^{n+1} = \Omega_{\rm f}^n + \delta t \boldsymbol{w}^{n+1}$ with

$$\tilde{\boldsymbol{\eta}}^{n+1} = \boldsymbol{\eta}^n + \delta t \left(\frac{3}{2} \boldsymbol{v}_{\rm s}{}^n - \frac{1}{2} \boldsymbol{v}_{\rm s}{}^{n-1} \right), \quad \boldsymbol{w}^{n+1} = \frac{\tilde{\boldsymbol{\eta}}^{n+1} - \boldsymbol{\eta}^n}{\delta t} \quad \text{on } \widehat{\Sigma}, \qquad \boldsymbol{w}^{n+1} = \operatorname{Tr}^{-1}\big(\boldsymbol{w}^{n+1}_{|\Sigma}\big). \tag{4}$$

– **Step 2:** ALE-Advection–diffusion step (explicit coupling):

$$\begin{cases} \rho_{\rm f} \dfrac{\tilde{\boldsymbol{u}}^{n+1} - \boldsymbol{u}^n}{\delta t}\bigg|_{\hat{x}} + \rho_{\rm f}\big(\tilde{\boldsymbol{u}}^n - \boldsymbol{w}^{n+1}\big) \cdot \nabla \tilde{\boldsymbol{u}}^{n+1} - \mu \Delta \tilde{\boldsymbol{u}}^{n+1} = 0, & \text{in } \Omega_{\rm f}^{n+1}, \\ \tilde{\boldsymbol{u}}^{n+1} = \boldsymbol{w}^{n+1}, & \text{on } \Sigma^{n+1}. \end{cases} \tag{5}$$

– **Step 3:** Projection step (implicit coupling):

$$\begin{cases} \rho_{\rm f} \dfrac{\boldsymbol{u}^{n+1} - \tilde{\boldsymbol{u}}^{n+1}}{\delta t} + \nabla p^{n+1} = 0 \quad \text{in } \Omega_{\rm f}^{n+1}, \quad \operatorname{div} \boldsymbol{u}^{n+1} = 0 \quad \text{in } \Omega_{\rm f}^{n+1}, \\ \boldsymbol{u}^{n+1} \cdot \boldsymbol{n}_{\rm f} = \dfrac{\boldsymbol{\eta}^{n+1} - \boldsymbol{\eta}^n}{\delta t} \cdot \boldsymbol{n}_{\rm f} \quad \text{on } \Sigma^{n+1}, \end{cases} \tag{6}$$

$$\begin{cases} \rho_{\rm s} \dfrac{\boldsymbol{v}_{\rm s}{}^{n+1} - \boldsymbol{v}_{\rm s}{}^n}{\delta t} - \operatorname{div}_{\hat{x}}\left(\dfrac{\boldsymbol{\Pi}^n + \boldsymbol{\Pi}^{n+1}}{2} \right) = 0 \quad \text{in } \widehat{\Omega}_{\rm s}, \quad \dfrac{\boldsymbol{\eta}^{n+1} - \boldsymbol{\eta}^n}{\delta t} = \dfrac{\boldsymbol{v}_{\rm s}{}^{n+1} + \boldsymbol{v}_{\rm s}{}^n}{2} \quad \text{in } \widehat{\Omega}_{\rm s}, \\ \boldsymbol{\Pi}^{n+1} \cdot \boldsymbol{n}_{\rm s} = J^{n+1}\big(\boldsymbol{\sigma}_{\rm f}\big(p^{n+1}, \tilde{\boldsymbol{u}}^{n+1}\big) \circ A^{n+1}\big)\big(\boldsymbol{F}^{n+1}\big)^{-\rm T} \cdot \boldsymbol{n}_{\rm s} \quad \text{on } \widehat{\Sigma}. \end{cases} \tag{7}$$

Variants of the above scheme can be obtained by switching steps 2 and 3, i.e. using a velocity-correction scheme within the fluid, or using incremental approaches [8].

We now state a stability result, whose proof can be found in [4], for our semi-implicit scheme (5)–(7) applied to a linearized version of problem (2), (3), where we have neglected the convective and geometrical non-linearities. As suggested by [7], the explicit treatment of the viscous sub-step leads to a conditionally stable scheme. The structure

is discretized in time using a Leap–Frog scheme. We consider Lagrange finite elements in space, for both the fluid and the structure, based on quasi-uniform triangulations, with h and H the fluid and solid mesh sizes, respectively. In addition, π_h represents a given matching operator at the interface.

Theorem 2.1. *Assume that the interface matching operator π_h is L^2-stable. Then, the linearized version of scheme* (5)–(7)*, is stable* (*in the energy norm*) *under the following condition*:

$$\rho_s \geqslant C\left(\rho_f \frac{h}{H^\alpha} + 2\frac{\mu\delta t}{hH^\alpha}\right), \quad \text{with } \alpha \overset{\text{def}}{=} \begin{cases} 0, & \text{if } \overline{\widehat{\Omega}}_s = \widehat{\Sigma}, \\ 1, & \text{if } \overline{\widehat{\Omega}}_s \neq \widehat{\Sigma} \end{cases} \tag{8}$$

with $C > 0$ a constant independent of the physical and discretization parameters.

Some remarks are in order:

- The assumption on the L^2-stability of the interface matching operator is satisfied by the standard finite element interpolation operator, for example, whenever the fluid interface triangulation is a sub-triangulation of the solid interface triangulation. This includes, in particular, the case of interface matching meshes. By construction, a mortar based matching operator also fulfills that assumption.
- Under a strong added-mass effect, condition (8) can be satisfied by reducing the ratios h/H^α and $\delta t/(hH^\alpha)$. The later might be thought as a CFL-like condition.
- In the case $\alpha = 0$, condition (8) becomes independent of the solid mesh size H. In particular, we may set $H = h$, and stabilize the scheme by simply reducing h (and δt).
- In the case $\alpha = 1$, the stability of the scheme can be ensured provided that the fluid mesh size h is small enough compared to the structure mesh size H. In the hemodynamic context, 3D numerical simulations showed however that this condition seems to be not necessary.

For further discussions on the stability of the scheme we refer to [4].

3. Numerical results

We consider the backward facing step with an elastic bottom wall Σ (Fig. 1). The wall displacement $\boldsymbol{\eta}$ is supposed to be along the Oy axis, and its vertical component, η, governed by the following equation

$$\rho_s \varepsilon_s \frac{\partial^2 \eta}{\partial t^2} - \alpha \frac{\partial^2 \eta}{\partial z^2} + \beta\eta - \gamma \frac{\partial^3 \eta}{\partial z^2 \partial t} = \boldsymbol{f}_\Sigma \cdot \boldsymbol{e}_y,$$

where $\boldsymbol{f}_\Sigma$ denotes the fluid load (pressure and viscous effects) on Σ, ε_s stands for the structure thickness and the coefficients α, β and γ are given constitutive constants. This model is purely illustrative and we do not discuss here its mechanical relevance. The values used in our simulations were $\alpha = 16.7$, $\beta = 26.7$, $\gamma = 0.1$. The product $\rho_s\varepsilon_s$ will be either 20 or 30 depending on the test case. The fluid is governed by the incompressible Navier–Stokes equations (2) with $\rho_f = 1$, $\mu = 0.01$. We impose the velocity $\boldsymbol{u} = (u_x, 0)$, with

$$u_x(y,t) = \frac{1}{4}\left(1 - \cos\left(\frac{\pi t}{2}\right)\right)(y-1)(2-y),$$

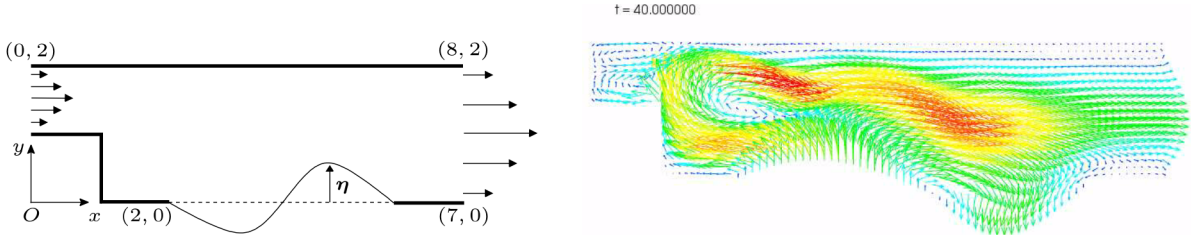

Fig. 1. Left: Backward facing step with an elastic bottom. Right: Example of the velocity field.

Fig. 1. À gauche : écoulement sur une marche avec fond élastique. À droite : exemple de champs de vitesse.

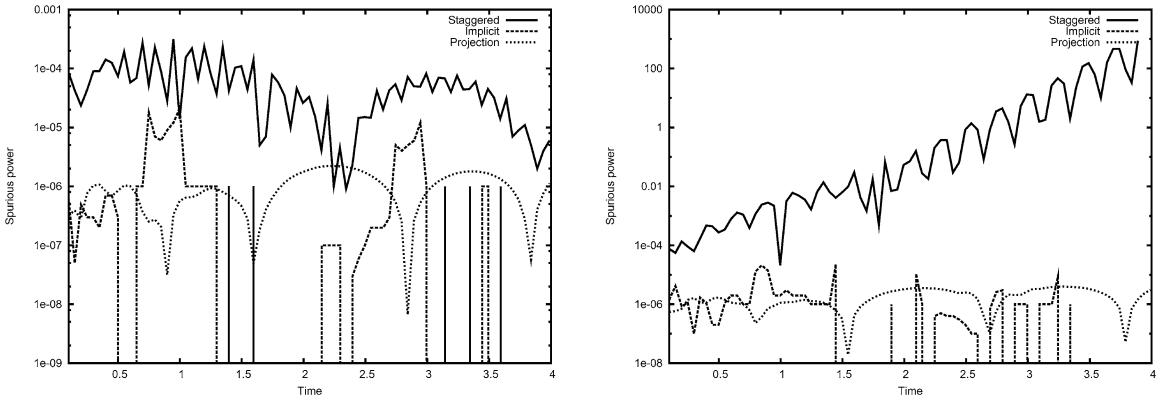

Fig. 2. Left: Spurious interface power (log scale) *versus* time for $\rho_s \varepsilon_s = 30$. Right: Spurious interface power (log scale) *versus* time for $\rho_s \varepsilon_s = 20$. The staggered scheme generates too much spurious power and is unstable in this case, while projection and implicit schemes remain stable.

Fig. 2. À gauche : puissance parasite à travers l'interface (échelle logarithmique) en fonction du temps pour $\rho_s \varepsilon_s = 30$. À droite : puissance parasite à travers l'interface (échelle logarithmique) en fonction du temps pour $\rho_s \varepsilon_s = 20$. Le schéma décalé génère trop d'énergie parasite et est instable dans ce cas, tandis que le schéma de projection et le schéma implicite demeurent stables.

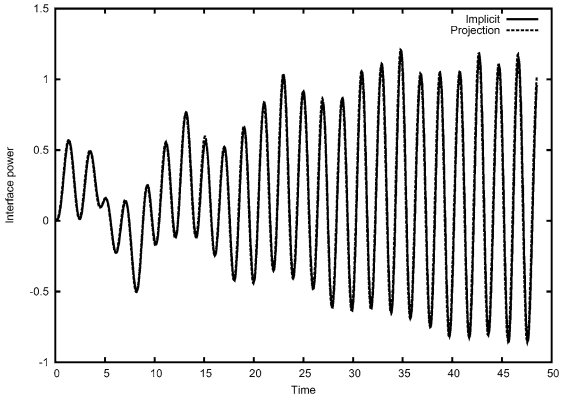

Fig. 3. Power transmitted across the fluid–structure interface versus time for $\rho_s \varepsilon_s = 20$. Observe the very good fitting between the projection and implicit schemes.

Fig. 3. Puissance transmise à travers l'interface fluide–structure en fonction du temps pour $\rho_s \varepsilon_s = 20$. Noter que les résultats obtenus avec le schéma implicite et le schéma de projection sont très proches.

on the inlet ($x = 0$), homogeneous Neumann boundary conditions on the outlet ($x = 8$), and a no-slip boundary condition anywhere else. The time step is $\delta t = 0.05$. The fluid equations are discretized using $\mathbb{Q}_2/\mathbb{Q}_1$ finite elements (1600 nodes), and the structure with $\mathbb{P}_1$ finite elements (50 nodes). In particular, we have $h = H = 0.1$. Fig. 1 shows an example of the velocity field.

We compare the projection scheme (4)–(7) with a fully implicit coupling (solved through inexact Newton iterations [6]), and a staggered scheme (with a second order prediction of the interface position). We monitor the power transmitted through the fluid–structure interface by the fluid and by the structure at the end of each time step. Fig. 2 shows the sum of this two quantities (which represents a spurious numerical power) *versus* time in a semi-log scale. The staggered scheme is stable for $\rho_s \varepsilon_s = 30$ (Fig. 2(left)). But it generates too much spurious power and is unstable whenever the added-mass effect increases, for example, when $\rho_s h_s = 20$ (Fig. 2(right)). For the implicit and the projection schemes, the spurious power is of order 10^{-5}, which is the tolerance used for the iterative algorithms. Fig. 3 points out that the interface powers obtained with the fully implicit and the projection schemes are very close. Other test cases, related to blood flows, will be reported in a forthcoming paper [4].

References

[1] P. Causin, J.-F. Gerbeau, F. Nobile, Added-mass effect in the design of partitioned algorithms for fluid–structure problems, Comput. Methods Appl. Mech. Engrg. 194 (42–44) (2005) 4506–4527.
[2] S. Deparis, M. Discacciati, G. Fourestey, A. Quarteroni, Heterogeneous domain decomposition methods for fluid–structure interaction problems, Technical report, EPFL-IACS report 08.2005, 2005.
[3] C. Farhat, K. van der Zee, Ph. Geuzaine, Provably second-order time-accurate loosely-coupled solution algorithms for transient nonlinear aeroelasticity, Comput. Methods Appl. Mech. Engrg., in press.
[4] M.A. Fernández, J.-F. Gerbeau, C. Grandmont, A projection semi-implicit scheme for the coupling of an elastic structure with an incompressible fluid, Technical Report 5700, INRIA, 2005, Int. J. Numer. Methods Engrg., submitted for publication.
[5] M.A. Fernández, M. Moubachir, A Newton method using exact Jacobians for solving fluid–structure coupling, Comput. & Structures 83 (2005) 127–142.
[6] J.-F. Gerbeau, M. Vidrascu, A quasi-Newton algorithm based on a reduced model for fluid–structure interactions problems in blood flows, Math. Model. Numer. Anal. 37 (4) (2003) 631–648.
[7] C. Grandmont, V. Guimet, Y. Maday, Numerical analysis of some decoupling techniques for the approximation of the unsteady fluid structure interaction, Math. Models Methods Appl. Sci. 11 (8) (2001) 1349–1377.
[8] J.-L. Guermond, P. Minev, J. Shen, An overview of projection methods for incompressible flows, Comput. Methods Appl. Mech. Engrg., submitted for publication.
[9] P. Le Tallec, J. Mouro, Fluid structure interaction with large structural displacements, Comput. Methods Appl. Mech. Engrg. 190 (2001) 3039–3067.
[10] H.G. Matthies, J. Steindorf, Partitioned strong coupling algorithms for fluid–structure interaction, Comput. & Structures 81 (2003) 805–812.
[11] D.P. Mok, W.A. Wall, E. Ramm, Partitioned analysis approach for the transient, coupled response of viscous fluids and flexible structures, in: W. Wunderlich (Ed.), Proceedings of the European Conference on Computational Mechanics, ECCM'99, TU Munich, 1999.
[12] F. Nobile, Numerical approximation of fluid–structure interaction problems with application to haemodynamics, PhD thesis, EPFL, Switzerland, 2001.